https://doi.org/10.5194/cp-2024-42
Preprint. Discussion started: 20 June 2024

Climate of the Past Discussions

Orbital-scale climate dynamics impacts on Gzhelian peatland wildfire activity in the Ordos Basin

Wenxu Du[1], Dawei Lv[1*], Zhihui Zhang[1*], Munira Raji[2], Cuiyu Song[1], Luojing Wang[1], Zekuan Li[1], Kai Cao[1], Ruoxiang Yuan[1], Yuzhuang Sun[3]

[1] Shandong Provincial Key Laboratory of Depositional Mineralization and Sedimentary Minerals, College of Earth Sciences and Engineering, Shandong University of Science and Technology, Qingdao 266590, China

[2] Sustainable Earth Institute, University of Plymouth, Devon, United Kingdom

[3] College of Earth Science and Engineering, Hebei University of Engineering, Handan 056038, Heibei, China

*Corresponding author: College of Earth Sciences and Engineering, Shandong University of Science and Technology, Qingdao 266590, China.

E-mail addresses: lvdawei95@163.com (D. Lv), zhzhihui@sdust.edu.cn (Z. Zhang).

Abstract

The Carboniferous, an important coal-forming period in geological history, was characterized by extensive vegetation and high oxygen levels. Numerous wildfire evidence suggests that high frequency of wildfire occurred at that time, specifically in peatlands. However, the control mechanisms for changes in wildfire activity in peatlands during this period are still not clearly understood. In this study, evidence from the Gzhelian in the Ordos Basin, such as the inertinite/vitrinite (I/V) ratio, indicated the existence of different frequencies of wildfire activity at that time. The CaO/MgO and CaO/MgO • Al_2O_3 climate indicators revealed that high-frequency wildfires mainly occur in warm and humid climates. Based on former age constraints, we deduced that orbital cycles (long eccentricity) controlled the climate influence on peatland wildfires during

https://doi.org/10.5194/cp-2024-42
Preprint. Discussion started: 20 June 2024

Climate of the Past Discussions

the Gzhelian. When eccentricity was high, abundant sunshine and frequent rainfall led to warmer and more humid peatlands. The latter environments were more favourable for vegetation development, leading to increased fuel loads, which in turn led to more frequent wildfires. Moreover, the Gzhelian global wildfire records, showed that evidence of wildfire during this period was mainly located in areas with abundant tropical vegetation, supporting the view that wildfire activity during this period was mainly controlled by the fuel loads. Although Hg could be produced by peatland wildfires, but our results show that Hg was mainly from frequent volcanic activity during this period.

Keywords: Wildfire; Inertinite; Gzhelian; Hg; Long eccentricity

1. Introduction

In recent years, information about wildfires preserved in coal seams has been exposed (Robson et al., 2015; Hou et al., 2022; Zhang et al., 2022). The macerals in the pyrogenic inertinite (fossil charcoal in coal), such as fusinite, semifusinite, and inertodetrinite, have been widely used as direct evidence to demonstrate the occurrence of paleo-wildfires (Scott, 2010, 2022; Jasper et al., 2013; Belcher and Hudspith, 2017; Uhl et al., 2022; Shen et al., 2023). The Carboniferous through Permian were important coal-forming periods in geologic history where large deposits of coal developed (Berner, 2003). Although wildfires of the period have been somewhat summarized by previous authors (e.g., Scott, 2000; Glasspool and Scott, 2010; Glasspool et al. 2015; Jasper et al. 2021), there is a dearth of high-resolution wildfire records from the period. Glasspool et al. (2015) concluded from the analysis of the inertinite in coal that the frequency of wildfires during the Late Paleozoic was mainly due to the higher oxygen content in the atmosphere at that time. However, more detailed controlled factors for Carboniferous through Permian wildfires need to be improved.

Many researchers have found that changes in charcoal abundance in sediments indicate

https://doi.org/10.5194/cp-2024-42
Preprint. Discussion started: 20 June 2024

changes in orbital cycle forcing climate change, which in turn influences wildfire activity (Verardo and Ruddiman, 1996; Thevenon et al., 2004; Hao et al., 2020; Shi et al., 2020; Cheng et al., 2022). Daniau et al. (2013) found that the past 170 kyr of grassland wildfire activity in southern Africa has been controlled by precession. Zhang et al. (2020a, 2023) found that wildfire activity during the Early to Middle Jurassic was influenced by changes in long eccentricity (405 kyr) and the precession cycle. The orbital period (eccentricity, obliquity, and precession) forces climate change, thus affecting the amount and flammability of vegetation fuels to control wildfire activity (Zhou et al., 2023). The study of whether wildfire activity in Carboniferous to Permian peatlands was controlled by changes in orbital cycles is unclear. Late Carboniferous Gzhelian global wildfire records indicate that the wildfire records were all distributed in tropical climate zones. Tropical climate zones have abundant fuel accumulation and orbital cycle forcing wildfire activity may be more pronounced (DiMichele, 2014).

As the largest Late Carboniferous to Early Permian peat basin in China, the Ordos Basin contained a large amount of coal seams, which were preserved with numerous volcanic ashes and wildfire products in the coal seams (Wang, 2017; Xu et al., 2020; Zhao et al., 2023; Zhang et al., 2023a, 2023b). In this paper, the focus is on the No. 9 coal of the Yaogou Coal Mine in the Jungar Coalfield of the Ordos torder to understand the occurrence of the Late Carboniferous wildfires and the variation of burning temperatures. Employing the clear age constraints of the No.9 coal seam, the possible role of long eccentricity orbital cycle changes in driving wildfires by means of wildfire frequency and climate indicators at that time can be explored (Zhang et al., 2023a). Volcanic activity, frequent wildfires, and other causes can lead to Hg enrichment, and this study also explores the relationship between wildfire activity, volcanic activity, and Hg at that time, using changes in Hg content in No. 9 coal.

https://doi.org/10.5194/cp-2024-42
Preprint. Discussion started: 20 June 2024


Climate of the Past Discussions

2. Geological setting

The Ordos Basin, located at the western margin of the North China Craton, is the second largest terrestrial sedimentary basin in China (Ao et al., 2012; Zhang et al., 2023a). The Jungar Coalfield is in the southwestern part of the Inner Mongolia Autonomous Region of China and in the northeastern part of the Ordos Basin, which contains about 26.8 Gt of coal reserves, which is one of the richest coal reserves in northern China (Dai et al., 2006,2008,2012; Li et al., 2016). The coalfield contains coal-bearing sequences of the Carboniferous and Permian systems (Wang et al., 2011).

This study was conducted in the Yaogou Mine, in the northeastern part of the Jungar Coal Field (Fig. 1b). The coal-bearing sequences in the Yaogou Mine include the Benxi Formation, Taiyuan Formation, and Shanxi Formation, with a total thickness of 84~200 m (Zhang et al., 2023a). The Benxi Formation, with a total thickness of 84~200 m (Zhang et al., 2023a), lies unconformably on the Middle Ordovician Majiagou Formation, with a thickness of about 17~28 m. The Taiyuan Formation is underlying by the Benxi Formation. The Taiyuan Formation, with a thickness of about 31-75 m (average 58 m), conformably overlies the Benxi Formation. The Taiyuan Formation consists mainly of grey and gray-white quartz sandstone, siltstone, mudstone, and five coal beds marked from top to base as No. 6 to No. 10 (Fig. 1c) (Zhang et al., 2023a). Zhang et al. (2023a) determined by U-Pb zircon from altered volcanic ashes at the top and bottom of No. 9 coal that the Taiyuan Formation in this study area belongs to the Gzhelian stage of the Late Pennsylvanian. The Shanxi Formation with a thickness of about 35-97 m is mainly terrigenous coal-bearing clastic rocks, dominated by sandstones and coal seams (Zhang et al., 2023a).

https://doi.org/10.5194/cp-2024-42
Preprint. Discussion started: 20 June 2024

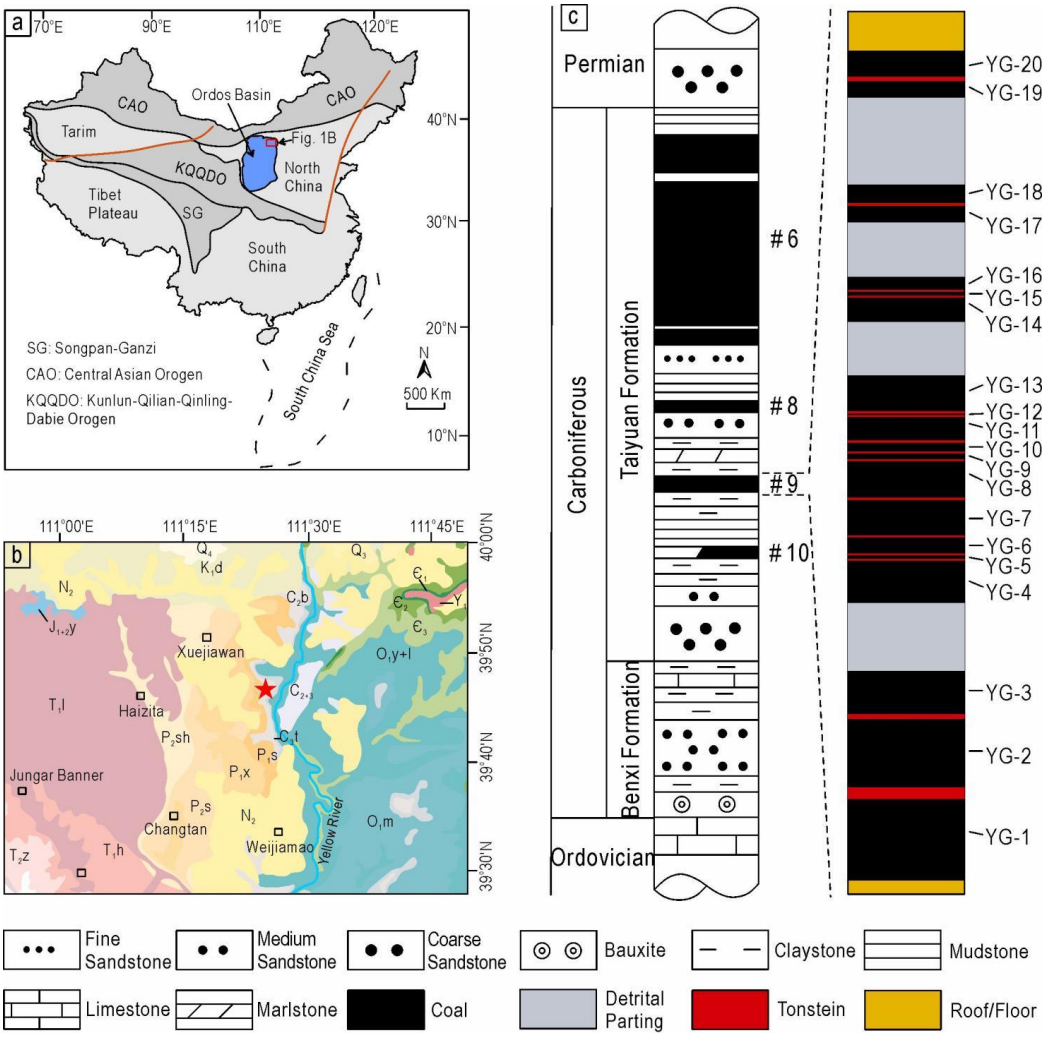

Fig. 1 Comprehensive geologic map of the Yaogou coal mine in the Ordos Basin, northern China. (a) Map showing the location of the Ordos Basin and the study area. (b) Geologic map of the study area showing the location of the study area (red stars). (c) Sedimentary sequence of the Jungar Coal Field and columnar map of the No. 9 coal seam. The No. 9 coal occurs in the Taiyuan Formation. Q_4-Holocene, Q_3-Pleistocene, N_2-Pliocene, K_1d-Dongsheng Formation (Fm.), $J_{1+2}y$-Yan'an Fm., T_2z-Zhifang Fm., T_1h-Heshanggou Fm., T_1l-Liujiagou Fm., P_2sh-Shiqianfeng Fm., P_2s-upper Shihezi Fm., P_1x-lower Shihezi Fm., P_1s-Shanxi Fm., C_3t-Taiyuan Fm., C_2b-Benxi Fm., O_1m-Majiagou Fm., O_1y+l-Yeli and Liangjiashan Formations. Figure modified from Zhang et al. (2023a).

https://doi.org/10.5194/cp-2024-42
Preprint. Discussion started: 20 June 2024

Climate of the Past Discussions

3. Material and methods

3.1 Sampling

In this study, a total of 20 coal samples were collected from the exposed face of the No. 9 coal at the Yaogou Mine, with a cumulative thickness of the profile of about 6.1 m. To minimize contamination and oxidation, the samples were all immediately stored in plastic bags. From bottom to top, all coal samples were marked YG-1 to YG-20 (Fig. 1c).

3.2 Analytical method

The analytical methods used in this study to demonstrate wildfire characteristics included petrographic analysis, coal rock micro component identification, fusinite reflectance measurements, and scanning electron microscopy (SEM).

The collected fossil charcoal fragments were crushed to a < 20 top size and the crushed samples were embedded in epoxy resins. The reflectance of the fusinite was measured by the oil immersion at room temperature and determined using an MSP UV-VIS2000 spectrophotometer (Petersen and Lindström, 2012; Xu et al., 2020). To estimate the wildfire burning temperatures represented by the experimental samples, calculations were based on the correlation proposed by previous works:

$$T=184.1+117.76\times\%R_o, \quad (1)$$

with R_o represents the reflectance of the inertinite (Jones, 1997; Petersen and Lindström, 2012). Based on the model of oxygen content proposed by Glasspool (2010, 2015), the oxygen content in the atmosphere was predicted for the period of this study:

$$I=(0.5-0.5\cos[\pi (O-O_{min})/(O_{max}-O_{min})])^n, \quad (2)$$

with I as the average inertinite content, O as the oxygen content, O_{max} as the oxygen content when the inertinite content reached 100%, and O_{min} as the oxygen content when was no inertinite.

https://doi.org/10.5194/cp-2024-42
Preprint. Discussion started: 20 June 2024

The microstructure of fossilized charcoal samples was observed by SEM to make a clearer observation of fossilized charcoal samples. The samples were observed under vacuum conditions using a 10 kV accelerating voltage, standard beam light, and a secondary electron probe. All the above experiments were completed at the Shandong Provincial Key Laboratory of Depositional Mineralisation and Sedimentary Minerals, Shandong University of Science and Technology.

To determine the coal rock components, the coal samples taken were measured according to the National Standard GB/T8899-2013. The reflectivity of the vitrinite group of the coal samples was measured according to the National Standard GB/T 6948-2008. To improve the quantification of charcoal abundance in each single sample, the ratio between inertinite maceral and vitrinite macerals (I/V), was calculated to determine the frequency of wildfires (Zhang et al., 2022). All of the latter experiments were completed in Xi'an Coal Science and Technology Ltd. All samples were analyzed for Total Organic Carbon (TOC) according to the National Standard GB/T19145-2003. All samples were analyzed for Hg concentration according to the National Standard GB/T 22105.1-2008. All above experiments were completed at the Beijing Qingchen Huanyu Petroleum Geological Technology Co. Ltd.

3.3 Data Synthesis

To build a reliable database of the Gzhelian wildfire evidence, data was compiled from peer-reviewed journal publications following the program of Lu (2021) and Lv (2024). Personal data and unpublished materials were not included in our study. We used the keywords ‘Gzhelian wildfire’, ‘charcoal’, ‘inertinite’, ‘fusain’, ‘fusinite’, and/or ‘PAHs’ to search papers in Google Scholar, Web of Science, ScienceDirect, and JSTOR. Literature searches were conducted by the end of April 2024.

To minimize the possibility of low credible/reliable wildfire data, the data published in the

https://doi.org/10.5194/cp-2024-42
Preprint. Discussion started: 20 June 2024


Climate of the Past Discussions

146 original article was double-checked and evaluated before inclusion in our database. The evidence
147 for fossil charcoal in the database is based on the standardized guidelines in Scott (2000,2010,2020).
148 The distinction between sources of PAHs (pyrogenic and petrogenic) was made according to Yunker
149 et al. (2002), and only records of pyrogenic PAHs were included. For example, Hower et al. (2022)
150 had two inertinite data that did not have details of where samples were taken, so they were
151 discarded. The inertinite in Presswood et al. (2016) was due to magmatic intrusion, so it was
152 discarded.

153 Three types of Gzhelian wildfire evidence were included in the database: charcoal type I
154 (pyrogenic inertinite macerals from coals), charcoal type II (fossil charcoal from clastic sediments),
155 and pyrogenic PAHs. The location (e.g., country, state/province, city, latitude, longitude, etc.),
156 palaeogeographical localities (e.g., palaeocontinents, palaeolatitude, and palaeolongitude),
157 stratigraphic unit (e.g., formation, group), and rock type (e.g., coal, sandstone, mudstone) were
158 integrated for each wildfire record. When multiple studies reported wildfire data from the same
159 geologic unit in the same location (e.g., section, region, or basin), they were considered as one
160 record (Lu et al., 2021). Depending on the type of evidence, wildfire occurrences in the same study
161 site can be identified in different studies and recorded as one occurrence.

162 The GPlates 2.2.0 model constructed by Scotece (2008) was used to estimate paleolatitudes
163 and paleolongitudes data for wildfire occurrence. To provide a visual representation of the spatial
164 distribution, the occurrence of wildfires was projected on a paleogeographic map of Gzhelian by
165 Scotese (2021) (Fig. 9).

166 ## 4. Results

167 ### *4.1 Coal rock micro component and geochemical characterization*

168 The microscopic component contents of the coal samples collected in the mineral-free state

https://doi.org/10.5194/cp-2024-42
Preprint. Discussion started: 20 June 2024


Climate of the Past Discussions

from No.9 coal of Yaogou Mine are shown in Table 1. Of all the samples, the vitrinite was dominant, with contents ranging from 64.5% to 84.7% (average = 73.5%). The inertinite content of the coal samples ranged from 14.1% to 30.8%, with an average content of 22.3%. The liptinite had the lowest content, ranging from 1.3% to 8.7%, with an average content of 4.2%. Nearly all inertinite preserved in coal was defined as an incomplete combustion product, comparable to fossil charcoal (Scott 2000, 2010; Scott and Glasspool 2006, 2007; Diessel, 2010). Because of this, subcomponent analyses were analyzed for the inertinite in the coal samples Table 1. In the 20 coal samples, the main component of the inertinite was semifusinite, with contents ranging from 7.4% to 17.2% with an average content of 11.5%. The content of inertodedetrinite was rather low, ranging from 1.8% to 13.4%, with an average content of 6.6%. The contents of fusinite, macrinite, and micrinite were low, with average contents of 1.2%, 2.3% and 0.7%. Among the 20 samples, the variation of inertinite/vitrinite ranged from 0.17 to 0.47, with a mean value of 0.31. The reflectance (R_{vo}) of the vitrinite of the 20 coal samples ranged from 0.37% to 0.66.

The TOC content of the 20 coal samples from the Taiyuan Formation ranged from 27.82% to 48.07%, with an average content of 39.49% (Table 2). The Hg content of the 20 samples varied greatly, ranging from 29.5 ppb to 393 ppb, with an average of 134.96 ppb (Table 2). Zhang et al. (2023a) analyzed the sulfur content, Al_2O_3 content, and ash yield of 20 coal seams in the Taiyuan Formation in this study area (Table 2). The Spearman correlation analysis showed that the correlation between Hg and Al_2O_3 in the 20 coal samples from Taiyuan Formation is highly significant, with positive correlation, the correlation coefficient is +0.529, and the significance is 0.016 (Fig. 6a). The correlation between Hg and sulfur is not significant with the correlation coefficient of -0.175 and significance of 0.46 (Fig. 6b). The correlation between Hg and TOC is significant, with a correlation coefficient of -0.659, and the significance is 0.002 (Fig. 6c). Since the

https://doi.org/10.5194/cp-2024-42
Preprint. Discussion started: 20 June 2024

Climate of the Past Discussions
Open Access
EGU

192 source of elemental aluminum in coal is mainly clay minerals, the correlation between elemental Al
193 and ash yield was analyzed. The correlation between elemental Al and ash yield in the coal samples
194 of this study was highly significant with a correlation coefficient of +0.776 and significance of 0.
195 The correlation between elemental Hg and ash yield was significant and positive with the
196 correlation coefficient of +0.481 and significance of 0.032 (Fig. 6d).

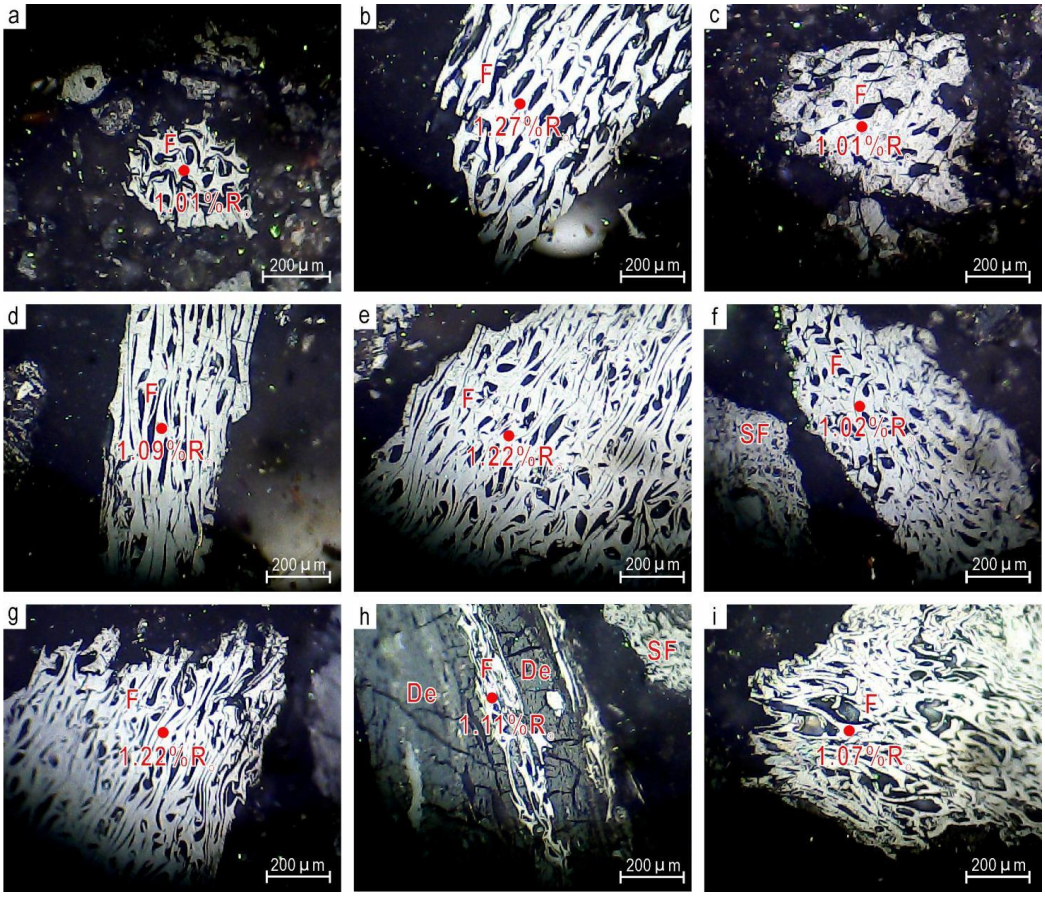

197

198 **Fig. 2** Features of fossil charcoal in the Ordos Basin Taiyuan Formation observed under the oil immersion optical
199 microscopy. F-fusinite; SF-semifusinite; Red circles show the test points, and numbers show the reflectance
200 values of the points.

https://doi.org/10.5194/cp-2024-42
Preprint. Discussion started: 20 June 2024

Climate of the Past Discussions

201 **Table 1**

202 The coal micro component contents of 20 seams of No. 9 coal from Yaogou Mine in Ordos Basin

Sample No.	Percentage of the total organic macerals (vol.%)			Percentage of the total inertinite macerals (vol.%)					TOM (vol.%)	Total minerals (vol.%)
	Vitrinite	Inertinite	Liptinite	Fusinite	Semifusinite	Macrinite	Micrinite	Inertodetrinite		
YG-1	79.6	14.6	5.8	1.1	9.3	0	0.2	4	53.9	46.1
YG-2	80.5	16	3.5	2.4	10.6	0.6	0.6	1.8	60.4	39.6
YG-3	68.3	27.4	4.3	0.9	14.1	1.5	2.6	8.3	81.2	18.8
YG-4	64.5	26.8	8.7	0.4	13.3	2.4	0.4	10.3	84.8	15.2
YG-5	84.7	11.9	3.4	0.4	7.4	1.5	0.2	2.4	84.9	15.1
YG-6	65.2	30.8	4	0	14.6	2.4	0.4	13.4	86.2	13.8
YG-7	72.2	23	4.8	3	10.7	3	0.8	5.5	87.1	12.9
YG-8	70.8	21.5	7.7	2.5	12.2	1.5	0.2	5.1	81.8	18.2
YG-9	78.4	19.1	2.5	0	9.8	2.5	0.4	6.4	80.1	19.9
YG-10	66.1	27.4	6.5	3.8	13.1	3.2	0.6	6.7	83.9	16.1
YG-11	75.2	23.5	1.3	0.6	12	3.4	0.2	7.3	79.6	20.4
YG-12	72.1	25.1	2.8	0.9	15.4	2.2	0.4	6.2	73.9	26.1
YG-13	65.8	30.2	4	0.8	17.2	4.1	1.8	6.3	86.2	13.8
YG-14	82	14.1	3.9	0	8.3	2.1	0	3.7	81.3	18.7
YG-15	80.2	18.4	1.4	0	11.2	0.8	0.6	5.8	77	23
YG-16	81.8	16.5	1.7	0	10.4	1.2	1.2	3.7	85.2	14.8
YG-17	78.1	18.4	3.5	2.7	9	1.7	0.5	4.5	59.5	40.5
YG-18	66.8	28.9	4.3	0.8	11.3	4.7	0	12.1	59.9	40.1
YG-19	73	24.9	2.1	1.1	8.9	2.9	0.4	11.6	71.5	28.5
YG-20	65	27.2	7.8	3.2	11	4.1	2	6.9	81.8	18.2

203

https://doi.org/10.5194/cp-2024-42
Preprint. Discussion started: 20 June 2024

Climate of the Past Discussions

Table 2

The chemical element data of 20 coal seams from the No. 9 coal of the Yaogou coal mine in the Ordos Basin. The Al_2O_3, TS, and TOC were from Zhang et al. (2023a).

Sample	Hg (ppb)	Al_2O_3 (%)	TS (%)	TOC (%)
YG-1	255	16.33	0.23	27.82
YG-2	145	11.94	0.39	29.92
YG-3	63.2	7.67	0.44	47.30
YG-4	118	9.46	0.77	44.14
YG-5	58.6	8.96	0.32	48.07
YG-6	70.4	12.75	0.41	42.04
YG-7	85.1	7.44	0.57	44.72
YG-8	35.4	7.42	0.52	48.04
YG-9	43.5	11.87	0.45	41.17
YG-10	269	10.5	0.59	41.51
YG-11	88.5	10.53	0.48	38.10
YG-12	83.9	10.74	0.5	35.33
YG-13	34.5	9.57	0.48	46.26
YG-14	156	12.77	0.35	40.37
YG-15	352	16.48	0.42	32.35
YG-16	237	14.23	0.32	36.72
YG-17	393	12.42	0.36	29.26
YG-18	152	17.88	0.29	32.05
YG-19	29.5	13.53	0.3	37.95
YG-20	29.6	7.57	0.44	46.68

4.2 Microscopic observations of fossil charcoal

Under the oil-immersion reflected-light microscope, a large amount of semifusinite was observed in the coal samples of the Taiyuan Formation. Some representative micrographs are provided in Fig. 2. The pore sizes of the semifusinite ranged from 40 - 120 μm , with a small variation in pore size. The measured reflectance of the inertinite of 20 coal samples from the Taiyuan Formation ranged from 1.01% to 2.07%, with the average value of 1.66%.

The structural features of the fibre structure and the cell wall in the fossil charcoal fragments can be observed by SEM. The majorityt of the cellular structures were crushed or broken(Fig. 3a,c). As shown by the radial structure, the tubular cells were straight and 10-20 μm wide (Fig. 3a). There was one single row of circular or elliptical pitting with 0.5-2 μm width (Fig. 3b). And the cell walls

https://doi.org/10.5194/cp-2024-42
Preprint. Discussion started: 20 June 2024

Climate of the Past Discussions
Open Access
EGU

of the samples showed homogenization (Fig. 3d).

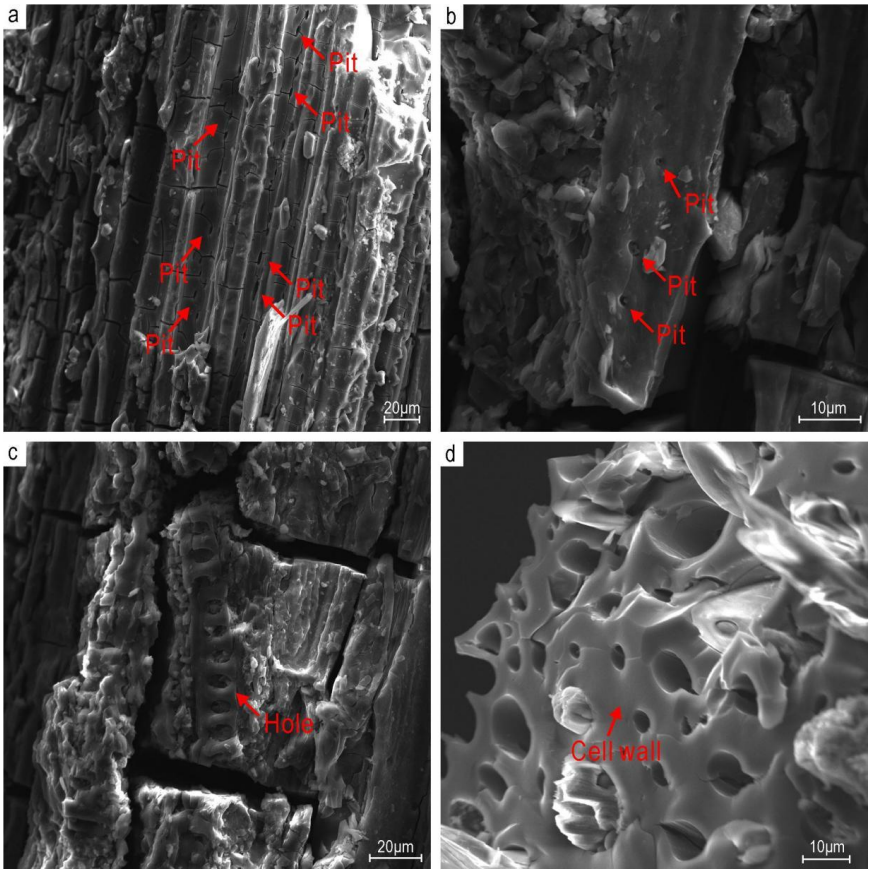

Fig. 3 Scanning electron microscope electron probe image of fossilized charcoal. (a-b) Red arrows point to uniseriate pits. (c) Red arrow points to larger holes in the cell wall that may represent pits, which were diagenetically enlarged during charring. (d) Red arrow points to homogenized cell wall.

4.3 The Gzhelian wildfire record in geologic context

Published wildfire records for the Gzhelian were compiled in Table S1. Based on the type of evidence these can be divided into five groups: 23 records of charcoal type I (79.4% of the total records), two records of charcoal type II (6.9%), one record of pyrogenic PAHs (3.4%), two records of charcoal type I and charcoal type II (6.9%), and one record of charcoal type II and pyrogenic PAHs (3.4%). The published Gzhelian wildfire data were observed in 19 geologic units (or

https://doi.org/10.5194/cp-2024-42
Preprint. Discussion started: 20 June 2024


Climate of the Past Discussions

formations), with two record from an unclear unit.

All of the 29 reported Gzhelian wildfires have occurred in the lower latitudes (30°N-30°S) (Fig. 9). According to Boucot et al.'s (2013) suggested paleoclimatic classification, the Gzhelian can be divided into four different paleoclimatic zones: cool temperate, warm temperate, arid and tropical. The Gzhelian wildfires all occurred in the tropical area (Fig. 9).

5. Discussion

5.1 Repeated wildfire in the Gzhelian of the Ordos Basin

The origin of the inertinite in coal has been controversial, and it has been suggested that the fusinite and semifusinite in the inertinite may be produced from fungal degradation of vegetation tissues in oxidizing environments or influenced by other microbial activities (Beeston, 1987; Teichmüller, 1989; Varma, 1996; ICCP, 2001). Some semifusinite in coal may also have been formed during diagenesis (Hudspith and Belcher, 2020). Nevertheless, research suggests that the fusinite and semifusinite in coal were equivalent to fossil charcoal (Scott and Glasspool, 2007; Hudspith et al., 2012), which was produced by the incomplete combustion of vegetation by wildfires (Scott, 2010; Liu et al., 2022). All coal samples from the Taiyuan Formation had low levels of both macrinite and micrinite (Table 1). Both fusinite and semifusinite preserved complete cellular structures (Fig. 2), suggesting that the fusinite and semifusinite in the study samples may be products of vegetation combustion.

In addition, the low reflectance of the vitrinite in the coal samples, averaging 0.49%, indicated that the samples were poorly metamorphosed, and was not enough to support the claim that the semifusinite in the samples was due to diagenesis. Experiments had shown that the carbonization temperature for homogenization of vegetation cell walls needs to be at least higher than 250 - 300 °C (Scott and Jones, 1991; Osterkamp et al., 2017). Obvious homogenization of the cell walls of the

https://doi.org/10.5194/cp-2024-42
Preprint. Discussion started: 20 June 2024


Climate of the Past Discussions

fossil charcoal could be observed under the SEM (Fig. 3d), which more clearly suggested that the fossil charcoal in the samples was caused by wildfire burning. The inertinite content of the Taiyuan Formation coal samples showed a small range of variability (14.1% - 30.8%) and was dominated by semifusinite (7.4% - 17.2%), which indicates the presence of frequent small wildfires during this period. Under the SEM, it can be observed that the cellular structure of the fossil charcoal from the Taiyuan Formation is obviously broken, and some cellular cavities in the charcoal appeared to have different degrees of deformation (Fig. 3c), which may be due to the tectonic movement of the strata.

Scott (2010) divided wildfires into three types based on their strength: surface fire, ground fire, and crown fire. Among these, surface fires whose fuels are mainly surface herbaceous, shrubs and various biological wastes, burn at lower temperatures, usually below 400 ºC. Ground fires whose fuel is mainly the dry humus layer in the soil, which can burn thick layers of peat, burn at relatively high temperatures, up to 600 ºC. It has been demonstrated that the reflectance of the inertinite is positively correlated with the combustion temperature, with higher inertinite reflectance indicating higher combustion temperatures (Jones et al., 1991; Guo and Bustin, 1998; Scott and Glasspool, 2007; McParland et al., 2009). The reflectance of the inertinite in the Taiyuan Formation samples varied in a small range (1.01%-2.07%), and it can be inferred that the Taiyuan Formation wildfire burned at temperatures ranging was about 300 ºC to 430 ºC, with an average burn temperature of 379 ºC (after formula Scott and Glasspool, 2015). This suggests that mainly low-temperature fires occurred in the Ordos Basin during the Gzhelian (Fig. 4). Wildfire burning may have been fueled primarily by low-growing vegetation or biological waste, which would be consistent with the homogenization of fern cell walls observed under the SEM.

https://doi.org/10.5194/cp-2024-42
Preprint. Discussion started: 20 June 2024

Climate of the Past Discussions
Open Access
EGU

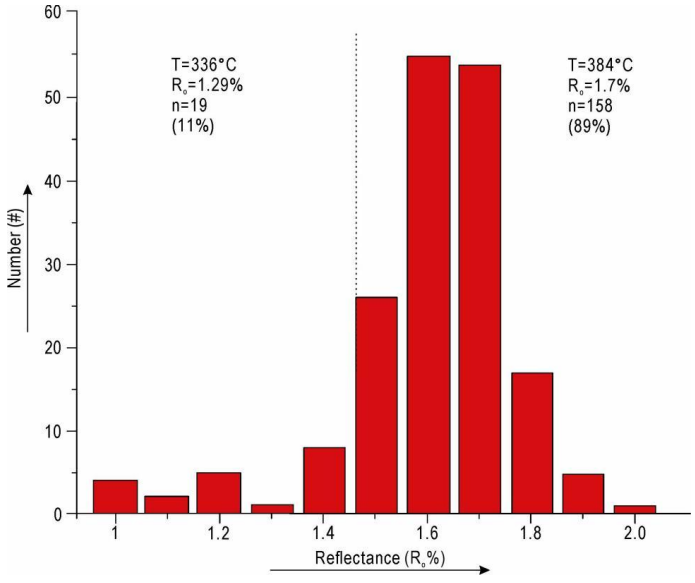

Fig. 4 The inertinite reflectance histograms indicate calculated combustion temperatures (Shukla et al., 2023).

5.2 Sources of elemental mercury in coal

Soils are the largest global reservoir of Hg and forest ecosystems are one of the key areas in the Hg cycle (Wang et al., 2019). Peatland vegetation can retain atmospheric Hg in their bodies by absorbing it (Grigal, 2003), while humus and sulfides in peatlands have a high affinity for Hg, which makes them important sinks for Hg (Yudovich and Ketris, 2005; Woerndle et al., 2018). In the pre-anthropic era, the main sources of Hg in the surface environment were volcanic eruptions, intense continental weathering, and wildfires (Pavlish et al., 2003; Pyle and Mather, 2003; Selin, 2009; Shen et al., 2020).

In this study, Hg was negatively correlated with Total Organic Carbon (TOC) and Total Sulfur (TS) (Fig. 6), indicating that Hg is not predominantly present in organic matter and sulfides. Correlation of elemental concentration with ash yield may provide preliminary information on their affinity with organic and inorganic (Eskanazy et al., 2010; Kortenski and Sotirov, 2002; Dai et al., 2012a; Zhang et al., 2023a). Mercury has a relatively high correlation (r=0.481) with ash yield, indicating a dominant inorganic affinity. There was a high correlation between Hg and Al_2O_3 in this

https://doi.org/10.5194/cp-2024-42
Preprint. Discussion started: 20 June 2024


Climate of the Past Discussions

study (r=0.529), indicating that Hg was mainly enriched in clay minerals (Fig. 6). The Hg concentrations in coal samples YG-1, YG-10, YG-15, YG-16, and YG-17 (237-352 ppb) were generally higher than the average concentration of coals from around the world (100 ppb) and the average concentration of Chinese coals (163 ppb) (Dai et al., 2012b). After normalizing for Al_2O_3, it still showed anomalously high values in these five coal samples, indicating that these five Hg peaks are true Hg anomalies (Fig. 5) (Xie et al., 2022).

Xie et al. (2022) demonstrated that wildfire burning resulted in the release of most of the Hg accumulated in vegetation and soils to the atmosphere, and that atmospheric Hg accumulated quickly in peatlands, leading to Hg anomalies enrichment in peatlands. Comparing the Hg levels of the samples in this study with the frequency of wildfires has not shown that the anomalously high values of Hg are well correlated with the frequency of wildfires (Fig. 5). There were even anomalously high values of Hg in samples YG-15, YG-16, and YG-17, but the frequency of wildfires was significantly reduced. This indicates that the anomalous enrichment of Hg in this study was not caused by wildfire burning.

The mass of Hg in forest vegetation is about 0.1 mg/m^2 , however, the mass of Hg in peatlands is about 20 mg/m^2 , which is much greater than the amount in vegetation (Grigal, 2003; Turetsky et al., 2006). The types of wildfire burning in Xie et al. (2022) were primarily ground and surface fires. Ground fires were fueled primarily by a dry humus layer in the soil (Scott, 2010), which can burn a thicker layer of peat, resulting in the release of Hg from the peatland. In this study, the type of wildfire burning was predominantly surface fires, with the primary fuels for surface fires were low surface vegetation and biological litter (Scott, 2010), which coincides with the observation of ferns as fuels in the SEM (Fig. 3). Ku et al. (2018) found that different wildfire intensities had different effects on Hg volatilization from vegetation. Therefore, wildfire burning may not necessarily lead to

https://doi.org/10.5194/cp-2024-42
Preprint. Discussion started: 20 June 2024

Hg enrichment, and wildfire types may not have the same effect on Hg. Mercury enrichment is favored when wildfires were primarily ground fires, where burning of the peat layer resulted in the release of large quantities of Hg, which were absorbed by the peatland.

Excluding the anomalous enrichment of Hg in coal due to wildfire activities, the known causes of the anomalous enrichment of Hg in coal are mainly the volcanic activities during the early peatland accretionary phase that led to the increase of Hg input (Roos-Barraclough et al., 2002; Yudovich and Ketris, 2005), and the invasion of low-temperature hydrothermal and magmatic fluids into coal-bearing strata (Sun et al., 2016; Zheng et al., 2018). Zhang et al. (2023a) identified 15 altered volcanic ashes in this study area, demonstrating the frequent volcanic activity during this depositional time. And it was confirmed that trace element enrichment in closed coal seams may be due to the dipping of tonsteins by acid solutions. Correlation analysis of the Hg content of No. 9 coal with trace elements such as Ga, Zr, and Hf revealed a significant correlation (r=0.581-0.705). Hg enrichment has been widely used as the indicator of volcanic sediment input (Shen et al., 2020), so the anomalously high values of Hg in the study area may be attributed to the input of Hg elements due to the frequent volcanic activities at that time, and the Hg in the tonsteins was leached into the closing coals by leaching of the acid solution.

https://doi.org/10.5194/cp-2024-42
Preprint. Discussion started: 20 June 2024

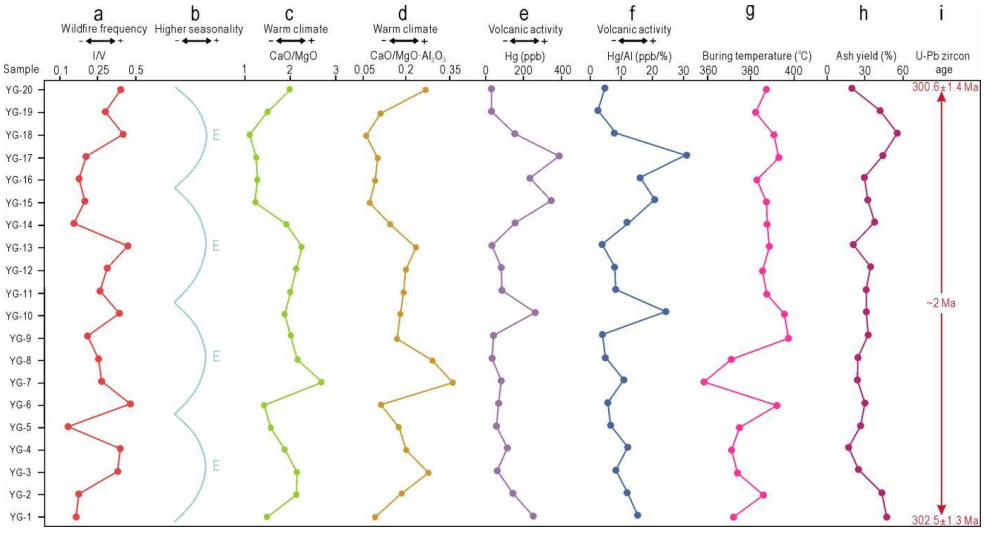

327

328 **Fig. 5** Comprehensive analysis map of No.9 coal in Yaogou Mine. (a) Inertinite/ Vitrinite variations in 20 coal

329 samples. (b) Long eccentricity orbital cycle variation. (c) CaO/MgO trends in 20 coal samples. (d)

330 CaO/MgO • Al_2O_3 trends in 20 coal samples. (e) Hg content trends in 20 coal samples. (f) Hg/Al trends in 20 coal

331 samples. (g) Combustion temperature trends in 20 coal samples. (h) Ash yield trends in 20 coal samples. (i) Age of

332 No. 9 coal, referred to Zhang et al. (2023a).

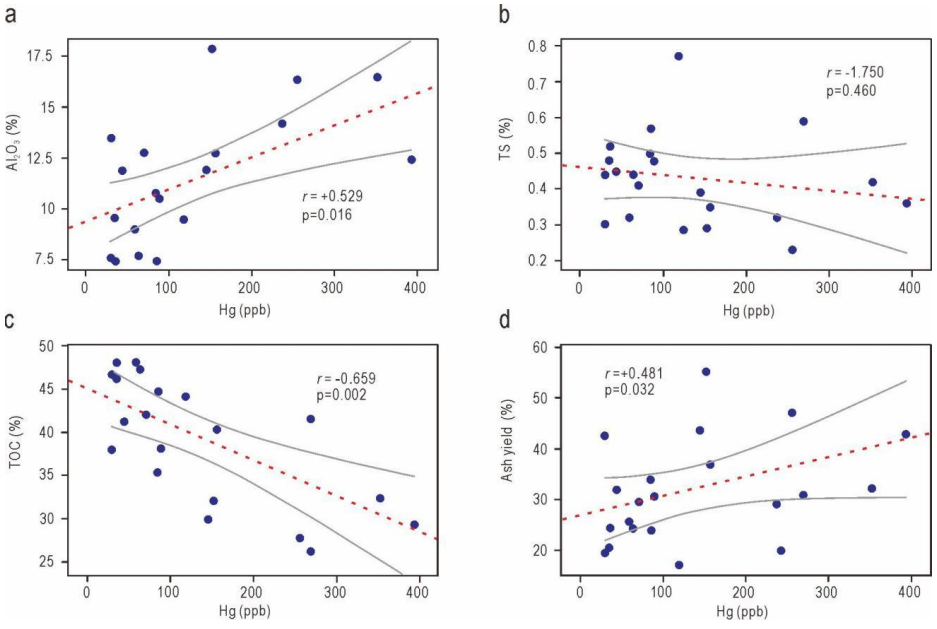

333

334 **Fig. 6** (a) Correlation between Hg and Al_2O_3. (b) Correlation between Hg and TS. (c) Correlation between Hg and

https://doi.org/10.5194/cp-2024-42
Preprint. Discussion started: 20 June 2024

335 TOC. (d) Correlation between Hg and ash yield. Spearman's P and r values are shown. Red lines denote the
336 best-fit linear regression line. Gray curve lines denote the 95% confidence interval.

337 ***5.3 Gzhelian wildfires and climate change***

338 ***5.3.1 Regional wildfire trends***

339 Wildfire activity during geologic history has been influenced primarily by changes in
340 atmospheric oxygen levels, climate and vegetation (Belcher and Hudspith, 2017; Baker, 2022). For
341 example, Glasspool and Scott (2010) suggested that high levels of oxygen in the atmosphere
342 influence increased wildfire activity on different time scales. Baker (2022) found that past periods
343 of global climate change on Earth have been accompanied by increased wildfire activity. Vegetation
344 type changes also influence wildfire occurrence, for example, the rise of angiosperms during the
345 Cretaceous may have led to an increase in wildfire activity at that time (Lü et al., 2024).

346 The level of oxygen in the atmosphere plays a key role in the occurrence of wildfires (Scott,
347 2000); when oxygen levels are below 15% it will not be possible to sustain vegetation burning, and
348 when levels are above 23% humid vegetation will continue to burn. Based on model predictions, the
349 oxygen level of 24.6% in the Gzhelian is higher than current oxygen levels and can sustain wildfire
350 burning in humidter environments (Fig. 7).

351 CaO/MgO can be used as an indicator for paleoclimate reconstruction (Chen and Wan, 1999;
352 Sun et al., 2010; Liu et al., 2013; Fu et al., 2018), and the ratio of CaO/MgO • Al_2O_3 can more
353 sensitively respond to the temperature changes at that time, with high values indicated for warm
354 periods, and low values indicated for cold periods (Chen and Wan, 1999; Fu et al., 2018; Zhang et
355 al., 2020b; Zhang et al., 2021). In this study, periods of high wildfire frequency (e.g., YG-10, YG-11,
356 YG-12, YG-13) had higher values of CaO/MgO and CaO/MgO • Al_2O_3, indicated of a warm and
357 humid climate (Fig. 5). Periods of lower wildfire frequency (e.g., YG-14, YG-15, YG-16, YG-17)

https://doi.org/10.5194/cp-2024-42
Preprint. Discussion started: 20 June 2024


Climate of the Past Discussions

had lower CaO/MgO and CaO/MgO • Al_2O_3 values, indicated a cold and dry climate (Fig. 5). Although wildfires were more easily caused when the climate was dry, cold climates with lower temperatures were not favourable for vegetation development (Brovkin, 2002), and a dryer climate meant less rainfall, both of which led to a decrease in fuels, hence a less frequent occurrence of wildfires. However, in warm and humid climatic periods, where seasonal variations were stronger, sufficient rainfall and suitable temperatures promote the development of vegetation, leading to a significant accumulation of fuels, hence more favourable for wildfires to occur (Litt et al., 2014; Stockhecke et al., 2016; Swain, 2021). Furthermore, previous research has found that high frequencies of wildfire activity have occurred in moderately humid environments (Daniau et al, 2012; Marlon et al, 2013). This study predicts oxygen levels sufficient to sustain wildfires in humid conditions for sustained burning, so sufficient fuel accumulation may have been a major factor in the frequency of wildfires during this period.

Many scholars have examined charcoal abundance changes in Quaternary sediments to show that orbital cycle forcing climate drives wildfire activity (Verardo and Ruddiman, 1996; Thevenon et al., 2004; Zhou et al., 2007; Daniau et al., 2013, 2023; Kappenberg et al., 2019; Hao et al., 2020; Shi et al., 2020; Zhang et al., 2023b). Zhou et al. (2023), based on a high-resolution charcoal fragment record from the Wushan Basin of the Tibetan Plateau during the Middle Miocene, found that orbital period (short eccentricity, slope, and age difference) forced climate change to control wildfire activity by influencing the amount of vegetative fuels and their combustibility. In this study, Coal 9 has a floor age of 300.6 ± 1.4 Ma, a roof age of 302.5 ± 1.3 Ma, and a depositional age of ~1.9 Ma (Zhang et al., 2023a). We explored the effect of the orbital cycle on wildfires using long eccentricity. As shown in Fig. 5(b-d), the variation of the long eccentricity had a good correlation with our climatic indicators (CaO/MgO, CaO/MgO • Al_2O_3). The maximum eccentricity is

https://doi.org/10.5194/cp-2024-42
Preprint. Discussion started: 20 June 2024

associated with a warmer and more humid period, while the minimum eccentricity is associated with a colder and dryer period. When the orbital cycle eccentricity is at maximum, the sun was at perihelion and the amount of insolation was relatively abundant, leading to a sufficient accumulation of fuels, which in turn led to an increase in wildfire activity (Kappenberg et al., 2019; Hollaar et al., 2021; Qiu et al., 2023; Zhang et al., 2023b). This is consistent with the study by Kappenberg et al. (2019) who found that orbital forcing leads to peak wildfire activity during warm and humid periods.

Combined with the above research, the factors controlling wildfires in this study area are shown in Fig. 8. When the eccentricity was at a minimum, the Earth received insufficient insolation, the climate was cold and dry, and seasonal variations were not evident (Hollaar et al., 2021; Huang et al., 2024). The lack of suitable environments for survival at that time resulted the low amount of vegetation. There may have been a low frequency of wildfires occurring at this stage, which produced less charcoal preserved in the peatland (Fig. 8a). When the eccentricity was at a maximum, the Earth received sufficient insolation, the climate was warm and humid, and seasonal variations were evident (Hollaar et al., 2021; Huang et al., 2024). Suitable environments lead to the proliferation of vegetation, which in turn accumulate large amounts of fuel. More rainfall was also followed by more lightning, leading to increased chances of ignition. Thus there were more frequent wildfires during the period, which produced more charcoal preserved in the peatlands (Fig. 8b). In this study, intensive wildfires did not correlate to peaks in Hg concentrations, and the anomalous enrichment of Hg was most likely due to the frequent volcanic activity occurring at that time. When the volcano erupts, the ash can carry large Hg transport (Coufalik et al., 2018). When volcanic ash passes through peatlands, the Hg it carried naturally settles and the strong adsorption of Hg by peatlands leads to anomalous enrichment of Hg at that time (Fig. 8a) (Yudovich and Ketris, 2005).

https://doi.org/10.5194/cp-2024-42
Preprint. Discussion started: 20 June 2024

Climate of the Past Discussions
Open Access
EGU

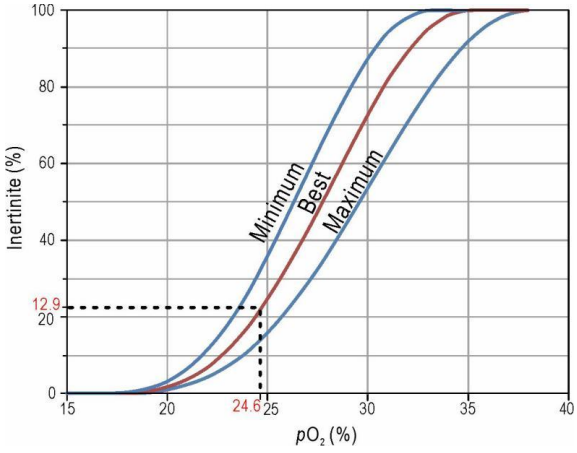

404

405 **Fig. 7** The atmospheric oxygen concentration during the Late Carboniferous Taiyuan Formation in the Ordos

406 Basin based on the prediction model proposed by Glasspool et al. (2015).

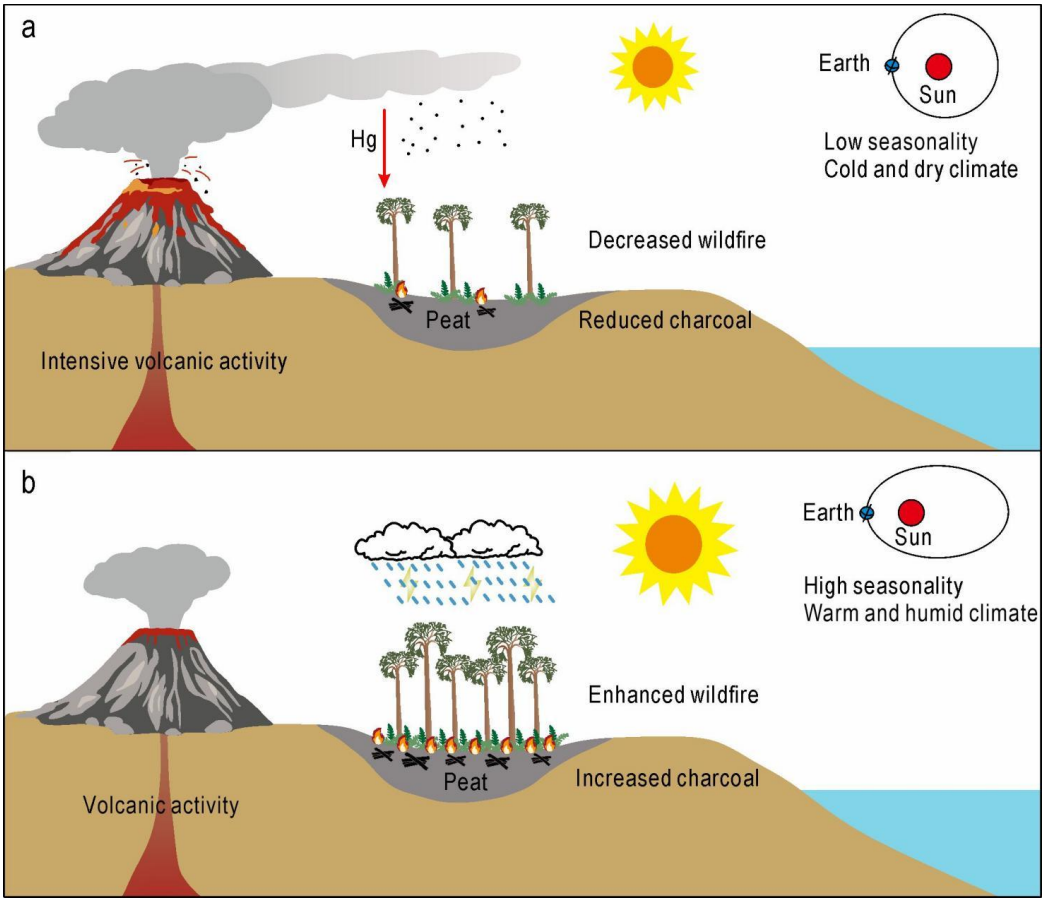

407

408 **Fig. 8** Illusrtation of wildfires activity forced by the long eccentricity orbital cycle in the study area.

https://doi.org/10.5194/cp-2024-42
Preprint. Discussion started: 20 June 2024

409 ***5.3.2 The geographical distribution of published evidence in the Gzhelian***

410 The distribution of wildfires on Earth is not random, and the spatial distribution of wildfires in
411 the modern world is affected by vegetation, climate, topography, and human activities (Krawchuk et
412 al., 2009). Studies have shown that frequent wildfires in modern environments mainly occur in
413 tropical forests and savannas (Mouillot and Field, 2005; Giglio et al., 2006; Flannigan et al., 2009,
414 2013). In this study, based on the distribution of climate zones published by Boucot et al. (2013), it
415 was found that all of the wildfire records for the Gzhelian occurred in the tropical climate zone (Fig.
416 9). It was similar to the modern distribution of wildfires. In the tropics of the Gzhelian, different
417 biomes are distributed, mainly divided into humid to semi-humid wetland groups and semi-humid
418 to semi-arid wetland groups, and the peatlands were under alternating humid and dry changing
419 environments (DiMichele et al., 2010; DiMichele, 2014). In warm and humid environments,
420 vegetation grows densely and generates large fuel accumulations. And in arid environments, fuel
421 burnability is enhanced, which in turn promotes more frequent wildfires (Denis et al., 2017; Baker,
422 2022). Hence the frequent occurrence of wildfires in the tropics with alternating seasons.

423 In view of the spatial distribution, the Gzhelian wildfire records were all located at low
424 latitudes near the equator. In the Gzhelian, the southern part of the Gondwana was covered by a
425 large ice sheet, resulting in the lack of vegetation and the lack of fuel needed for wildfires to burn
426 (Scotese, 2021) (Fig. 9). Similarly in the northern part of the Gondwana and the northern part of the
427 Laurasia there were extensive arid climate zones spread across the mainland that lacked the fuels
428 needed for wildfire burning, resulting in the absence of wildfire records (Fig. 9). However, it is
429 worth noting that widespread biases, such as taphonomy, research preferences, and sampling bias,
430 may result in global wildfire data for the Gzhelian not representing the true situation at that time
431 (Brown et al., 2012; Hamad et al., 2012; Lu et al., 2021; Lü et al., 2024). For example, this study

https://doi.org/10.5194/cp-2024-42
Preprint. Discussion started: 20 June 2024

Climate of the Past Discussions
Open Access
EGU

found no evidence of wildfires that have been reported in warm temperate regions (Fig. 9).

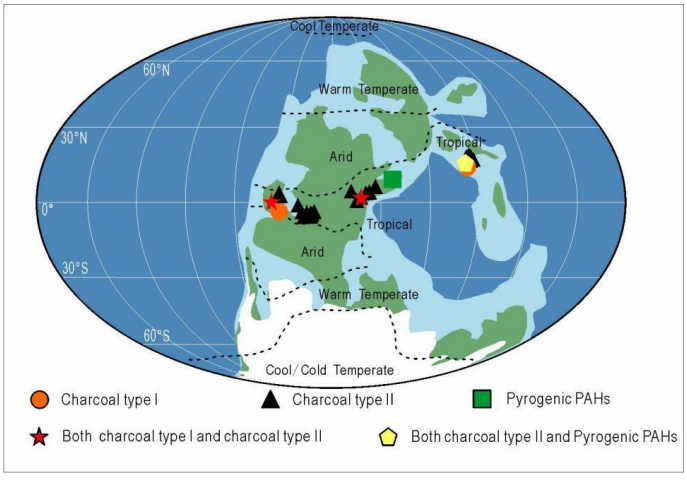

Fig. 9 Paleogeographic distribution of published wildfire occurrences during the Gzhelian. Plate reconstructions from Scotese (2016) with paleoclimatic zones based on Boucot et al. (2013).

6. Conclusion

In this study, the detailed analysis of the inertinite in the No. 9 coal of the Yaogou coal mine in the Ordos Basin, China, demonstrated that frequent wildfires had occurred in the region during the Gzhelian of the Late Carboniferous and were mainly low-temperature fires. The frequency of wildfires during this period may be related to the forcing of the long eccentricity orbital cycle, where changes in the climate due to changes in the orbital cycle affect the fuel load. The review of the global wildfire record of the Gzhelian that wildfires were concentrated in low-latitude tropical climates, and the distribution of wildfires may have been limited by the climate and fuels available at that time. The anomalous enrichment of Hg in No. 9 coal was probably due to inputs of Hg from the frequent volcanic activity occurring at that time, and was not related to wildfire burning. The different types of wildfire burning may limit the release and enrichment of Hg.

Author Contribution

All the authors have actively participated in the preparation of the manuscript. Wenxu Du was

449 responsible for data curation, methodology, and writing; Dawei Lv was responsible for funding
450 acquisition, project administration, and supervision; Zhihui Zhang was responsible for funding
451 acquisition and methodology; Munira Raji was responsible for review; Cuiyu Song was responsible
452 for conceptualization and methodology; Luojing Wang was responsible for visualization and
453 investigation; Zekuan Li was responsible for investigation; Kai Cao was responsible for software
454 and validation; Ruoxiang Yuan was responsible for visualization and investigation; Yuzhuang Sun
455 was responsible for review. All authors read and approved the final proof.

456 ## Competing Interests

457 The authors declare that they have no conflict of interest.

458 ## Acknowledgement

459 This work was financially supported by the National Natural Science Foundation of China
460 (Grant No. 42102127) and the Natural Science Foundation of Shandong Province (Grant No.
461 ZR2021QD087), Shandong University of Science and Technology (Grant No. 2018TDJH101). We
462 think the Deep-Time Digital Earth program (DDE) to support this work. We thank Jincheng Xu to
463 helped with this study. We gratefully acknowledge Professor James C. Hower for his valuable
464 comments on this paper.

465 ## References

466 Ao, W., Huang, W., Weng, C., Xiao, X., Liu, D., Tang, X., Chen, P., Zhao, Z., Wan, H., and
467 Finkelman, R. B.: Coal petrology and genesis of Jurassic coal in the Ordos Basin, China,
468 Geoscience Frontiers, 3, 85-95, https://doi.org/10.1016/j.gsf.2011.09.004, 2012.
469 Baker, S. J.: Fossil evidence that increased wildfire activity occurs in tandem with periods of global
470 warming in Earth's past, Earth-Science Reviews, 224, 103871,
471 https://doi.org/10.1016/j.earscirev.2021.103871, 2022.

https://doi.org/10.5194/cp-2024-42
Preprint. Discussion started: 20 June 2024

472 Beeston, J.: Organic petrology of liptinites in the denison trough, Queensland, The APPEA Journal,
473 27, 86-97, https://doi.org/10.1071/AJ86009, 1987.
474 Belcher, C. M., and Hudspith, V. A.: Changes to Cretaceous surface fire behaviour influenced the
475 spread of the early angiosperms, New Phytologist, 213, 1521-1532,
476 https://doi.org/10.1111/nph.14264, 2017.
477 Berner, R. A.: The long-term carbon cycle, fossil fuels and atmospheric composition, Nature, 426,
478 323-326, https://doi.org/10.1038/nature02131, 2003.
479 Boucot, A. J., Xu, C., Scotese, C. R., and Morley, R. J.: Phanerozoic paleoclimate: an atlas of
480 lithologic indicators of climate, SEPM (Society for Sedimentary Geology) Tulsa, OK,
481 https://doi.org/10.2110/sepmcsp.11, 2013.
482 Brovkin, V.: Climate-vegetation interaction, Journal de Physique IV (Proceedings), 57-72,
483 https://doi.org/10.1051/jp4:20020452, 2002.
484 Brown, S. A., Scott, A. C., Glasspool, I. J., and Collinson, M. E.: Cretaceous wildfires and their
485 impact on the Earth system, Cretaceous research, 36, 162-190,
486 https://doi.org/10.1016/j.cretres.2012.02.008, 2012.
487 Carlquist, S., and Schneider, E. L.: Vessels in ferns: structural, ecological, and evolutionary
488 significance, American Journal of Botany, 88, 1-13, https://doi.org/10.2307/2657121, 2001.
489 Chen, J. a., and Wan, G.: Sediment particle size distribution and its environmental significance in
490 Lake Erhai, Yunnan Province, Chinese Journal of Geochemistry, 18, 314-320,
491 https://doi.org/10.1007/bf03052905, 1999.
492 Cheng, T., Zou, J., Shi, X., Gorbarenko, S., Vasilenko, Y., Bosin, A., Liu, Y., Chen, B., and Cheng,
493 F.: Climate-driven changes in high-intensity wildfire on orbital timescales in Eurasia since 320
494 Ka, Lithosphere, https://doi.org/10.2113/2022/7562666, 2022.

https://doi.org/10.5194/cp-2024-42
Preprint. Discussion started: 20 June 2024

Coufalík, P., Krmíček, L., Zvěřina, O., Meszarosová, N., Hladil, J., and Komárek, J.: Model of mercury flux associated with volcanic activity, Bulletin of environmental contamination and toxicology, 101, 549-553, https://doi.org/10.1007/s00128-018-2430-5, 2018.

Dai, S., Ren, D., Chou, C.-L., Li, S., and Jiang, Y.: Mineralogy and geochemistry of the no. 6 coal (Pennsylvanian) in the Junger Coalfield, Ordos Basin, China, International Journal of Coal Geology, 66, 253-270, https://doi.org/10.1016/j.coal.2005.08.003, 2006.

Dai, S., Li, D., Chou, C.-L., Zhao, L., Zhang, Y., Ren, D., Ma, Y., and Sun, Y.: Mineralogy and geochemistry of boehmite-rich coals: new insights from the Haerwusu Surface Mine, Jungar Coalfield, Inner Mongolia, China, International journal of coal geology, 74, 185-202, https://doi.org/10.1016/j.coal.2008.01.001, 2008.

Dai, S., Jiang, Y., Ward, C. R., Gu, L., Seredin, V. V., Liu, H., Zhou, D., Wang, X., Sun, Y., and Zou, J.: Mineralogical and geochemical compositions of the coal in the Guanbanwusu Mine, Inner Mongolia, China: Further evidence for the existence of an Al (Ga and REE) ore deposit in the Jungar Coalfield, International Journal of Coal Geology, 98, 10-40, https://doi.org/10.1016/j.coal.2012.03.003, 2012a.

Dai, S., Ren, D., Chou, C.-L., Finkelman, R. B., Seredin, V. V., and Zhou, Y.: Geochemistry of trace elements in Chinese coals: A review of abundances, genetic types, impacts on human health, and industrial utilization, International Journal of Coal Geology, 94, 3-21, https://doi.org/10.1016/j.coal.2011.02.003, 2012b.

Daniau, A.-L., Sánchez Goñi, M. F., Martinez, P., Urrego, D. H., Bout-Roumazeilles, V., Desprat, S., and Marlon, J. R.: Orbital-scale climate forcing of grassland burning in southern Africa, Proceedings of the National Academy of Sciences, 110, 5069-5073, https://doi.org/10.1073/pnas.1214292110, 2013.

https://doi.org/10.5194/cp-2024-42
Preprint. Discussion started: 20 June 2024

518 Daniau, A.-L., Loutre, M.-F., Swingedouw, D., Laepple, T., Bassinot, F., Malaizé, B., Kageyama,
519 M., Charlier, K., and Carfantan, H.: Precession and obliquity forcing of the South African
520 monsoon revealed by sub-tropical fires, Quaternary Science Reviews, 310, 108128,
521 https://doi.org/10.1016/j.quascirev.2023.108128, 2023.
522 Daniau, A. L., Bartlein, P. J., Harrison, S., Prentice, I. C., Brewer, S., Friedlingstein, P.,
523 Harrison-Prentice, T., Inoue, J., Izumi, K., and Marlon, J.: Predictability of biomass burning in
524 response to climate changes, Global Biogeochemical Cycles, 26,
525 https://doi.org/10.1029/2011GB004249, 2012.
526 Denis, E. H., Pedentchouk, N., Schouten, S., Pagani, M., and Freeman, K. H.: Fire and ecosystem
527 change in the Arctic across the Paleocene-Eocene Thermal Maximum, Earth and Planetary
528 Science Letters, 467, 149-156, https://doi.org/10.1016/j.epsl.2017.03.021, 2017.
529 Diessel, C. F.: The stratigraphic distribution of inertinite, International Journal of Coal Geology, 81,
530 251-268, https://doi.org/10.1016/j.coal.2009.04.004, 2010.
531 DiMichele, W. A., and Phillips, T. L.: The ecology of Paleozoic ferns, Review of Palaeobotany and
532 Palynology, 119, 143-159, https://doi.org/10.1016/s0034-6667(1)00134-8, 2002.
533 DiMichele, W. A.: Wetland-dryland vegetational dynamics in the Pennsylvanian ice age tropics,
534 International Journal of Plant Sciences, 175, 123-164, https://doi.org/10.1086/675235, 2014.
535 Eskanazy, G., Finkelman, R. B., and Chattarjee, S.: Some considerations concerning the use of
536 correlation coefficients and cluster analysis in interpreting coal geochemistry data,
537 International Journal of Coal Geology, 83, 491-493, https://doi.org/10.1016/j.coal.2010.05.006,
538 2010.
539 Flannigan, M., Cantin, A. S., De Groot, W. J., Wotton, M., Newbery, A., and Gowman, L. M.:
540 Global wildland fire season severity in the 21st century, Forest Ecology and Management, 294,

https://doi.org/10.5194/cp-2024-42
Preprint. Discussion started: 20 June 2024

54-61, https://doi.org/10.1016/j.foreco.2012.10.022, 2013.

Flannigan, M. D., Krawchuk, M. A., de Groot, W. J., Wotton, B. M., and Gowman, L. M.: Implications of changing climate for global wildland fire, International journal of wildland fire, 18, 483-507, https://doi.org/10.1071/wf08187, 2009.

Giglio, L., Van der Werf, G., Randerson, J., Collatz, G., and Kasibhatla, P.: Global estimation of burned area using MODIS active fire observations, Atmospheric Chemistry and Physics, 6, 957-974, https://doi.org/10.5194/acp-6-957-2006, 2006.

Glasspool, I. J., and Scott, A. C.: Phanerozoic concentrations of atmospheric oxygen reconstructed from sedimentary charcoal, Nature Geoscience, 3, 627-630, https://doi.org/10.1038/ngeo923, 2010.

Glasspool, I. J., Scott, A. C., Waltham, D., Pronina, N., and Shao, L.: The impact of fire on the Late Paleozoic Earth system, Frontiers in Plant Science, 6, 756, https://doi.org/10.3389/fpls.2015.00756, 2015.

Grigal, D.: Mercury sequestration in forests and peatlands: a review, Journal of environmental quality, 32, 393-405, https://doi.org/10.2134/jeq2003.0393, 2003.

Guo, Y., and Bustin, R.: FTIR spectroscopy and reflectance of modern charcoals and fungal decayed woods: implications for studies of inertinite in coals, International Journal of Coal Geology, 37, 29-53, https://doi.org/10.1016/s0166-5162（98）00019-6, 1998.

Hamad, A. M. A., Jasper, A., and Uhl, D.: The record of Triassic charcoal and other evidence for palaeo-wildfires: signal for atmospheric oxygen levels, taphonomic biases or lack of fuel?, International Journal of Coal Geology, 96, 60-71, https://doi.org/10.1016/j.coal.2012.03.006, 2012.

Hao, Y., Han, Y., An, Z., and Burr, G. S.: Climatic control of orbital time-scale wildfire occurrences

https://doi.org/10.5194/cp-2024-42
Preprint. Discussion started: 20 June 2024

564 since the late MIS 3 at Qinghai Lake, monsoon marginal zone, Quaternary international, 550,
565 20-26, https://doi.org/10.1016/j.quaint.2020.03.002, 2020.
566 Hollaar, T. P., Baker, S. J., Hesselbo, S. P., Deconinck, J.-F., Mander, L., Ruhl, M., and Belcher, C.
567 M.: Wildfire activity enhanced during phases of maximum orbital eccentricity and precessional
568 forcing in the Early Jurassic, Communications Earth & Environment, 2, 247,
569 https://doi.org/10.1038/s43247-021-00307-3, 2021.
570 Hou, H., Shao, L., Liang, G., Tang, Y., Zhang, H., and Zhang, J.: Repeated wildfires in the middle
571 jurassic Xishanyao formation (aalenian and bajocian ages) in northwestern China, Acta
572 Geologica Sinica-English Edition, 96, 1752-1763, https://doi.org/10.1111/1755-6724.14912,
573 2022.
574 Hower, J. C., Eble, C. F., Hopps, S. D., and Morgan, T. D.: Aspects of rare earth element
575 geochemistry of the Pond Creek coalbed, Pike County, Kentucky, International Journal of Coal
576 Geology, 261, 104082, https://doi.org/10.1016/j.coal.2022.104082, 2022.
577 Huang, H., Fang, Q., Huang, W., Shi, M., Zhang, S., Yang, T., Li, H., and Wu, H.: A short-term
578 warming interval during the apex of the late Paleozoic Ice Age: Evidence from geochemical
579 and magnetic records from South China, Palaeogeography, Palaeoclimatology, Palaeoecology,
580 112178, https://doi.org/10.1016/j.palaeo.2024.112178, 2024.
581 Hudspith, V., Scott, A., Collinson, M., Pronina, N., and Beeley, T.: Evaluating the extent to which
582 wildfire history can be interpreted from inertinite distribution in coal pillars: An example from
583 the Late Permian, Kuznetsk Basin, Russia, International Journal of Coal Geology, 89, 13-25,
584 https://doi.org/10.1016/j.coal.2011.07.009, 2012.
585 Hudspith, V. A., and Belcher, C. M.: Some semifusinite in coal may form during diagenesis, not
586 wildfires, International Journal of Coal Geology, 218, 103360,

https://doi.org/10.5194/cp-2024-42
Preprint. Discussion started: 20 June 2024

https://doi.org/10.1016/j.coal.2019.103360, 2020.

Jasper, A., Guerra-Sommer, M., Hamad, A. M. A., Bamford, M., Bernardes-de-Oliveira, M. E. C., Tewari, R., and Uhl, D.: The burning of Gondwana: Permian fires on the southern continent—A palaeobotanical approach, Gondwana Research, 24, 148-160, https://doi.org/10.1016/j.gr.2012.08.017, 2013.

Jasper, A., Pozzebon-Silva, Â., Carniere, J. S., and Uhl, D.: Palaeozoic and Mesozoic palaeo-wildfires: An overview on advances in the 21st Century, Journal of Palaeosciences, 70, 159-172, https://doi.org/10.54991/jop.2021.13, 2021.

Jinhua, F., Shixiang, L., Liming, X., and Xiaobing, N.: Paleo-sedimentary environmental restoration and its significance of Chang 7 Member of Triassic Yanchang Formation in Ordos Basin, NW China, Petroleum Exploration and Development, 45, 998-1008, https://doi.org/10.1016/s1876-3804（18）30104-6, 2018.

Jones, T. P., and Chaloner, W. G.: Fossil charcoal, its recognition and palaeoatmospheric significance, Palaeogeography, Palaeoclimatology, Palaeoecology, 97, 39-50, https://doi.org/10.1016/0031-0182（91）90180-y, 1991.

Jones, T. P.: Fusain in late jurassic sediments from the witch ground graben, North sea, UK, in: 4th European Palaeobotanical and Palynological Conference, Heerlen/Kerkrade, The Netherlands, 19-23 September 1994, 99-104, 1997.

Kappenberg, A., Lehndorff, E., Pickarski, N., Litt, T., and Amelung, W.: Solar controls of fire events during the past 600,000 years, Quaternary Science Reviews, 208, 97-104, https://doi.org/10.1016/j.quascirev.2019.02.008, 2019.

Kortenski, J., and Sotirov, A.: Trace and major element content and distribution in Neogene lignite from the Sofia Basin, Bulgaria, International Journal of Coal Geology, 52, 63-82,

https://doi.org/10.5194/cp-2024-42
Preprint. Discussion started: 20 June 2024

https://doi.org/10.1016/s0166-5162(02)00133-7, 2002.

Krawchuk, M. A., Moritz, M. A., Parisien, M.-A., Van Dorn, J., and Hayhoe, K.: Global pyrogeography: the current and future distribution of wildfire, PloS one, 4, e5102, https://doi.org/10.1371/journal.pone.0005102, 2009.

Ku, P., Tsui, M. T.-K., Nie, X., Chen, H., Hoang, T. C., Blum, J. D., Dahlgren, R. A., and Chow, A. T.: Origin, reactivity, and bioavailability of mercury in wildfire ash, Environmental science & technology, 52, 14149-14157, https://doi.org/10.1021/acs.est.8b03729, 2018.

Li, Y., Tang, D., Wu, P., Niu, X., Wang, K., Qiao, P., and Wang, Z.: Continuous unconventional natural gas accumulations of Carboniferous-Permian coal-bearing strata in the Linxing area, northeastern Ordos basin, China, Journal of Natural Gas Science and Engineering, 36, 314-327, https://doi.org/10.1016/j.jngse.2016.10.037, 2016.

Litt, T., Pickarski, N., Heumann, G., Stockhecke, M., and Tzedakis, P. C.: A 600,000 year long continental pollen record from Lake Van, eastern Anatolia (Turkey), Quaternary Science Reviews, 104, 30-41, https://doi.org/10.1016/j.quascirev.2014.03.017, 2014.

Liu, B., Jin, H., Sun, L., Sun, Z., and Su, Z.: Winter and summer monsoonal evolution in northeastern Qinghai-Tibetan Plateau during the Holocene period, Geochemistry, 73, 309-321, https://doi.org/10.1016/j.chemer.2013.03.006, 2013.

Liu, B., Spiekermann, R., Zhao, C., Puettmann, W., Sun, Y., Jasper, A., and Uhl, D.: Evidence for the repeated occurrence of wildfires in an upper Pliocene lignite deposit from Yunnan, SW China, International Journal of Coal Geology, 250, 103924, https://doi.org/10.1016/j.coal.2021.103924, 2022.

Lü, D.-W., Du, W.-X., Zhang, Z.-H., Gao, Y., Wang, T.-T., Xu, J.-C., Zhang, A.-C., and Wang, C.-S.: A synthesis of the Cretaceous wildfire record related to atmospheric oxygen levels?, Journal of

https://doi.org/10.5194/cp-2024-42
Preprint. Discussion started: 20 June 2024

633 Palaeogeography, 13, 149-164, https://doi.org/10.1016/j.jop.2023.10.001, 2024.
634 Lu, M., Ikejiri, T., and Lu, Y.: A synthesis of the Devonian wildfire record: Implications for
635 paleogeography, fossil flora, and paleoclimate, Palaeogeography, Palaeoclimatology,
636 Palaeoecology, 571, 110321, https://doi.org/10.1016/j.palaeo.2021.110321, 2021.
637 Marlon, J. R., Bartlein, P. J., Daniau, A.-L., Harrison, S. P., Maezumi, S. Y., Power, M. J., Tinner, W.,
638 and Vanniére, B.: Global biomass burning: a synthesis and review of Holocene paleofire
639 records and their controls, Quaternary Science Reviews, 65, 5-25,
640 https://doi.org/10.1016/j.quascirev.2012.11.029, 2013.
641 McParland, L. C., Collinson, M. E., Scott, A. C., and Campbell, G.: The use of reflectance values
642 for the interpretation of natural and anthropogenic charcoal assemblages, Archaeological and
643 Anthropological Sciences, 1, 249-261, https://doi.org/10.1007/s12520-009-0018-z, 2009.
644 Mouillot, F., and Field, C. B.: Fire history and the global carbon budget: a 1 × 1 fire history
645 reconstruction for the 20th century, Global Change Biology, 11, 398-420,
646 https://doi.org/10.1111/j.1365-2486.2005.00920.x, 2005.
647 Osterkamp, I. C., Lara, D. M. d., Gonçalves, T. A. P., Kauffmann, M., Périco, E., Stülp, S.,
648 Machado, N. T. G., Uhl, D., and Jasper, A.: Changes of wood anatomical characters of selected
649 species of Araucaria-during artificial charring-implications for palaeontology, Acta Botanica
650 Brasilica, 32, 198-211, https://doi.org/10.1590/0102-33062017abb0360, 2017.
651 Pavlish, J. H., Sondreal, E. A., Mann, M. D., Olson, E. S., Galbreath, K. C., Laudal, D. L., and
652 Benson, S. A.: Status review of mercury control options for coal-fired power plants, Fuel
653 processing technology, 82, 89-165, https://doi.org/10.1016/S0378-3820（03）00059-6, 2003.
654 Petersen, H. I., and Lindström, S.: Synchronous wildfire activity rise and mire deforestation at the
655 Triassic-Jurassic boundary, https://doi.org/10.1371/journal.pone.0047236, 2012.

https://doi.org/10.5194/cp-2024-42
Preprint. Discussion started: 20 June 2024

656 Presswood, S. M., Rimmer, S. M., Anderson, K. B., and Filiberto, J.: Geochemical and petrographic
657 alteration of rapidly heated coals from the Herrin (No. 6) Coal Seam, Illinois Basin,
658 International Journal of Coal Geology, 165, 243-256,
659 https://doi.org/10.1016/j.coal.2016.08.022, 2016.
660 Pyle, D. M., and Mather, T. A.: The importance of volcanic emissions for the global atmospheric
661 mercury cycle, Atmospheric Environment, 37, 5115-5124,
662 https://doi.org/10.1016/j.atmosenv.2003.07.011, 2003.
663 Qiu, R., Fang, L., Lv, P., Jiang, F., Zhang, X., Zhang, X., Zhang, P., Zhu, L., and Shi, S.: Long
664 eccentricity forcing of the Late Pliensbachian to Early Toarcian (Jurassic) terrestrial wildfire
665 activities in the Tarim Basin, northwestern China, Palaeogeography, Palaeoclimatology,
666 Palaeoecology, 613, 111408, https://doi.org/10.1016/j.palaeo.2023.111408, 2023.
667 Robson, B. E., Collinson, M. E., Riegel, W., Wilde, V., Scott, A. C., and Pancost, R. D.: Early
668 Paleogene wildfires in peat-forming environments at Schöningen, Germany, Palaeogeography,
669 Palaeoclimatology, Palaeoecology, 437, 53-62, https://doi.org/10.1016/j.palaeo.2015.07.016,
670 2015.
671 Roos-Barraclough, F., Martinez-Cortizas, A., García-Rodeja, E., and Shotyk, W.: A 14 500 year
672 record of the accumulation of atmospheric mercury in peat: volcanic signals, anthropogenic
673 influences and a correlation to bromine accumulation, Earth and Planetary Science Letters, 202,
674 435-451, https://doi.org/10.1016/s0012-821x（02）00805-1, 2002.
675 Schneider, E. L., and Carlquist, S.: SEM studies on vessels in ferns. 17. Psilotaceae, American
676 Journal of Botany, 87, 176-181, https://doi.org/10.2307/2656903, 2000.
677 Scotese, C.: The PALEOMAP Project PaleoAtlas for ArcGIS, version 1, Volume, 2, 16-31, 2008.
678 Scotese, C. R.: An atlas of Phanerozoic paleogeographic maps: the seas come in and the seas go out,

https://doi.org/10.5194/cp-2024-42
Preprint. Discussion started: 20 June 2024

679 Annual Review of Earth and Planetary Sciences, 49, 679-728,
680 https://doi.org/10.1146/annurev-earth-081320-064052, 2021.
681 Scott, A. C., and Jones, T. P.: Fossil charcoal: a plant-fossil record preserved by fire, Geology Today,
682 7, 214-216, https://doi.org/10.1111/j.1365-2451.1991.tb00806.x, 1991.
683 Scott, A. C.: The Pre-Quaternary history of fire, Palaeogeography, palaeoclimatology,
684 palaeoecology, 164, 281-329, https://doi.org/10.1016/s0031-0182（00）00192-9, 2000.
685 Scott, A. C., and Glasspool, I. J.: The diversification of Paleozoic fire systems and fluctuations in
686 atmospheric oxygen concentration, Proceedings of the National Academy of Sciences, 103,
687 10861-10865, https://doi.org/10.1073/pnas.0604090103, 2006.
688 Scott, A. C., and Glasspool, I. J.: Observations and experiments on the origin and formation of
689 inertinite group macerals, International Journal of Coal Geology, 70, 53-66,
690 https://doi.org/10.1016/j.coal.2006.02.009, 2007.
691 Scott, A. C.: Charcoal recognition, taphonomy and uses in palaeoenvironmental analysis,
692 Palaeogeography, Palaeoclimatology, Palaeoecology, 291, 11-39,
693 https://doi.org/10.1016/j.palaeo.2009.12.012, 2010.
694 Scott, A. C.: Fire: A Very Short Introduction, Oxford University Press, Great Clarendon Street,
695 Oxford, OX2 6DP,United Kingdom, https://doi.org/10.1093/actrade/9780198830030.001.0001,
696 2020.
697 Scott, A. C.: Charcoalified vegetation from the Pennsylvanian of Yorkshire, England: Implications
698 for the interpretation of Carboniferous wildfires, Review of Palaeobotany and Palynology, 296,
699 https://doi.org/10.1016/j.revpalbo.2021.104540, 104540, 2022.
700 Selin, N. E.: Global biogeochemical cycling of mercury: a review, Annual review of environment
701 and resources, 34, 43-63, https://doi.org/10.1146/annurev.environ.051308.084314, 2009.

https://doi.org/10.5194/cp-2024-42
Preprint. Discussion started: 20 June 2024

Shen, J., Feng, Q., Algeo, T. J., Liu, J., Zhou, C., Wei, W., Liu, J., Them II, T. R., Gill, B. C., and Chen, J.: Sedimentary host phases of mercury (Hg) and implications for use of Hg as a volcanic proxy, Earth and Planetary Science Letters, 543, 116333, https://doi.org/10.1016/j.epsl.2020.116333, 2020.

Shen, W., Zhao, Q., Uhl, D., Wang, J., and Sun, Y.: Wildfire activity and impacts on palaeoenvironments during the late Paleozoic Ice Age-New data from the North China Basin, Palaeogeography, Palaeoclimatology, Palaeoecology, 629, 111781, https://doi.org/10.1016/j.palaeo.2023.111781, 2023.

Shi, Y., Pan, B., Wei, M., Li, X., Cai, M., Wang, J., Xu, X., Hu, J., and Shi, W.: Wildfire evolution and response to climate change in the Yinchuan Basin during the past 1.5 Ma based on the charcoal records of the PL02 core, Quaternary Science Reviews, 241, 106393, https://doi.org/10.1016/j.quascirev.2020.106393, 2020.

Stockhecke, M., Timmermann, A., Kipfer, R., Haug, G. H., Kwiecien, O., Friedrich, T., Menviel, L., Litt, T., Pickarski, N., and Anselmetti, F. S.: Millennial to orbital-scale variations of drought intensity in the Eastern Mediterranean, Quaternary Science Reviews, 133, 77-95, https://doi.org/10.1016/j.quascirev.2015.12.016, 2016.

Sun, Q., Wang, S., Zhou, J., Chen, Z., Shen, J., Xie, X., Wu, F., and Chen, P.: Sediment geochemistry of Lake Daihai, north-central China: implications for catchment weathering and climate change during the Holocene, Journal of Paleolimnology, 43, 75-87, https://doi.org/10.1007/s10933-009-9315-x, 2010.

Sun, R., Sonke, J. E., and Liu, G.: Biogeochemical controls on mercury stable isotope compositions of world coal deposits: A review, Earth-science reviews, 152, 1-13, https://doi.org/10.1016/j.earscirev.2015.11.005, 2016.

https://doi.org/10.5194/cp-2024-42
Preprint. Discussion started: 20 June 2024

725 Swain, D. L.: A shorter, sharper rainy season amplifies California wildfire risk, Geophysical
726 Research Letters, 48, e2021GL092843, https://doi.org/10.1029/2021gl092843, 2021.
727 Teichmüller, M.: The genesis of coal from the viewpoint of coal petrology, International Journal of
728 Coal Geology, 12, 1-87, https://doi.org/10.1016/0166-5162（89）90047-5, 1989.
729 Thevenon, F., Bard, E., Williamson, D., and Beaufort, L.: A biomass burning record from the West
730 Equatorial Pacific over the last 360 ky: methodological, climatic and anthropic implications,
731 Palaeogeography, Palaeoclimatology, Palaeoecology, 213, 83-99,
732 https://doi.org/10.1016/s0031-0182（04）00364-5, 2004.
733 Turetsky, M. R., Harden, J. W., Friedli, H. R., Flannigan, M., Payne, N., Crock, J., and Radke, L.:
734 Wildfires threaten mercury stocks in northern soils, Geophysical research letters, 33,
735 https://doi.org/10.1029/2005gl025595, 2006.
736 Uhl, D., Spiekermann, R., Wuttke, M., Poschmann, M. J., and Jasper, A.: Wildfires during the
737 Paleogene (late Eocene – late Oligocene) of the Neuwied Basin (W-Germany), Review of
738 Palaeobotany and Palynology, 297, 104565, https://doi.org/10.1016/j.revpalbo.2021.104565,
739 2022.
740 Varma, A.: Influence of petrographical composition on coking behavior of inertinite-rich coals,
741 International journal of coal geology, 30, 337-347, https://doi.org/10.1016/0166-5162（95）
742 00053-4, 1996.
743 Verardo, D. J., and Ruddiman, W. F.: Late Pleistocene charcoal in tropical Atlantic deep-sea
744 sediments: climatic and geochemical significance, Geology, 24, 855-857,
745 https://doi.org/10.1130/0091-7613（1996）024<0855：LPCITA>2.3.co;2, 1996.
746 Wang, C. a., Liu, Y., Zhang, X., and Che, D.: A study on coal properties and combustion
747 characteristics of blended coals in northwestern China, Energy & Fuels, 25, 3634-3645,

https://doi.org/10.5194/cp-2024-42
Preprint. Discussion started: 20 June 2024

https://doi.org/10.1021/ef200686d, 2011.

Wang, S.: Ordos basin superposed evolution and structural controls of coal forming activities, Earth Science Frontiers, 24, 54-63, https://10.13745/j.esf.yx.2016-12-11, 2017. (in Chinese).

Wang, X., Yuan, W., Lin, C.-J., Zhang, L., Zhang, H., and Feng, X.: Climate and vegetation as primary drivers for global mercury storage in surface soil, Environmental Science & Technology, 53, 10665-10675, https://doi.org/10.1021/acs.est.9b02386, 2019.

Woerndle, G. E., Tsz-Ki Tsui, M., Sebestyen, S. D., Blum, J. D., Nie, X., and Kolka, R. K.: New insights on ecosystem mercury cycling revealed by stable isotopes of mercury in water flowing from a headwater peatland catchment, Environmental science & technology, 52, 1854-1861, https://doi.org/10.1021/acs.est.7b04449, 2018.

Xie, W., Tan, J., Wang, W., Jia, J., Liu, Z., Wu, J., Wang, Y., and Song, X.: Record of Middle Jurassic wildfire and its incidental mercury emissions in northern Qaidam Basin, China: Evidence from the inertinite and mercury anomalies in coal, International Journal of Coal Geology, 261, 104078, https://doi.org/10.2139/ssrn.4105730, 2022.

Xu, Y., Uhl, D., Zhang, N., Zhao, C., Qin, S., Liang, H., and Sun, Y.: Evidence of widespread wildfires in coal seams from the Middle Jurassic of Northwest China and its impact on paleoclimate, Palaeogeography, Palaeoclimatology, Palaeoecology, 559, 109819, https://doi.org/10.1016/j.palaeo.2020.109819, 2020.

Yudovich, Y. E., and Ketris, M.: Mercury in coal: A review: Part 1. Geochemistry, International Journal of Coal Geology, 62, 107-134, https://doi.org/10.1016/s0140-6701（06）81438-4, 2005.

Yunker, M. B., Macdonald, R. W., Vingarzan, R., Mitchell, R. H., Goyette, D., and Sylvestre, S.: PAHs in the Fraser River basin: a critical appraisal of PAH ratios as indicators of PAH source and composition, Organic geochemistry, 33, 489-515, https://doi.org/10.1016/s0146-6380（02）

https://doi.org/10.5194/cp-2024-42
Preprint. Discussion started: 20 June 2024

00002-5, 2002.

Zhang, X., Li, S., Zhao, X., Geng, G., and Yan, M.: The sedimentary environment of Early Cretaceous rift basin in eastern China and its response to the Faraoni event, Geosciences Journal, 24, 359-377, https://doi.org/10.1007/s12303-019-0031-x, 2020a.

Zhang, X., Gao, Z., Fan, T., Xue, J., Li, W., Cao, F., and Zhang, H.: Geochemical characteristics, provenance and paleodepostional environment of the Lower Jurassic Huxishan Formation in the Lenghu area, northwestern Qaidam Basin, North West China: Implications for organic matter origin, Journal of Petroleum Science and Engineering, 205, 108951, https://doi.org/10.1016/j.petrol.2021.108951, 2021.

Zhang, Z.-H., Lü, D.-W., Wang, T.-T., An, D.-Z., Liu, H.-Y., Wang, D.-D., and Wang, C.-S.: Intensive peatland wildfires during the Aptian-Albian oceanic anoxic event 1b: Evidence from borehole SK-2 in the Songliao Basin, NE China, Journal of Palaeogeography, 11, 448-467, https://doi.org/10.1016/j.jop.2022.06.002, 2022.

Zhang, Z., Wang, C., Lv, D., Hay, W. W., Wang, T., and Cao, S.: Precession-scale climate forcing of peatland wildfires during the early middle Jurassic greenhouse period, Global and planetary change, 184, 103051, https://doi.org/10.1016/j.gloplacha.2019.103051, 2020b.

Zhang, Z., Lv, D., Hower, J. C., Wang, L., Shen, Y., Zhang, A., Xu, J., and Gao, J.: Geochronology, mineralogy, and geochemistry of tonsteins from the Pennsylvanian Taiyuan Formation of the Jungar Coalfield, Ordos Basin, North China, International Journal of Coal Geology, 267, 104183, https://doi.org/10.1016/j.coal.2023.104183, 2023a.

Zhang, Z., Lv, D., Lu, M., Yu, Z., Gao, Y., Wang, T., Gao, J., and Wang, C.: Wildfire activity driven by the 405-kyr orbital climate cycles in the Middle Jurassic, Global and Planetary Change, 222, 104069, https://doi.org/10.1016/j.gloplacha.2023.104069, 2023b.

https://doi.org/10.5194/cp-2024-42
Preprint. Discussion started: 20 June 2024

794 Zhao, C., Zhang, K., Xiao, L., Uhl, D., Shi, Z., Zhao, W., Zhao, Q., Sun, Y., and Liu, B.:
795 Paleoclimate-induced wildfires in a paleomire in the Ordos Basin, Northern China during the
796 Middle Jurassic greenhouse period, Chemical Geology, 637, 121677,
797 https://doi.org/10.1016/j.chemgeo.2023.121677, 2023.
798 Zheng, L., Sun, R., Hintelmann, H., Zhu, J., Wang, R., and Sonke, J. E.: Mercury stable isotope
799 compositions in magmatic-affected coal deposits: New insights to mercury sources, migration
800 and enrichment, Chemical Geology, 479, 86-101,
801 https://doi.org/10.1016/j.chemgeo.2017.12.032, 2018.
802 Zhou, B., Shen, C., Sun, W., Zheng, H., Yang, Y., Sun, Y., and An, Z.: Elemental carbon record of
803 paleofire history on the Chinese Loess Plateau during the last 420 ka and its response to
804 environmental and climate changes, Palaeogeography, Palaeoclimatology, Palaeoecology, 252,
805 617-625, https://doi.org/10.1016/j.palaeo.2007.05.014, 2007.
806 Zhou, X., Hui, Z., Vachula, R. S., Wei, X., Chen, P., Zhang, J., Wang, X., and Peng, T.:
807 Mid-Miocene palaeofire and its complex relationship with vegetation changes in the Wushan
808 Basin, northeastern Tibetan Plateau, China: Evidence from a high-resolution charcoal record,
809 Paleoceanography and Paleoclimatology, 38, e2022PA004461,
810 https://doi.org/10.1029/2022pa004461, 2023.